The influence of gas diffusion on bubble persistence in shock-scattering histotripsy

Kenneth B. Bader[a)]
Department of Radiology and the Committee on Medical Physics, University of Chicago, Chicago, Illinois 60637, USA
baderk@uchicago.edu

Viktor Bollen
Department of Radiology, University of Chicago, Chicago, Illinois 60637, USA
bollen@uchicago.edu

Abstract: Bubble cloud persistence reduces the efficacy of mechanical liquefaction with shock-scattering histotripsy. In this study, the contribution of gas transfer to bubble longevity was investigated *in silico* by solving the equations for bubble oscillations and diffusion in parallel. The bubble gas content increased more than 5 orders of magnitude during the expansion phase, arresting the inertial collapse. The residual gas bubble required more than 15 ms for passive dissolution post excitation, consistent with experimental observation. These results demonstrate gas diffusion is an important factor in the persistence of histotripsy-induced cavitation.

[CCC]
Date Received: March 16, 2018 **Date Accepted:** May 31, 2018

1. Introduction

Shock-scattering histotripsy is a focused ultrasound therapy under development for tissue liquefaction.[1] Unlike thermal ultrasound therapies, shock-scattering histotripsy relies on the formation of a bubble cloud to ablate tissue.[2] Bubbles thought to be nucleated from nanoscale sources expand tens of micrometers in diameter under the tensile phase of the histotripsy pulse.[3] Bubble clouds can persist for more than 50 ms after the acoustic excitation pulse,[4–6] even in highly degassed media. Persistent bubbles shield the focal zone from subsequent pulses, preventing complete liquefaction of the target tissues. One potential mechanism for the bubble persistence is gas diffusion. *In silico* computations denote that the bubble dynamics in a fluid medium are influenced by gas diffusion for shock wave lithotripsy[7] and boiling histotripsy[8] excitations. Diffusion may also play a role in shock-scattering histotripsy bubble activity initiated in an elastic medium. In this study, the response of a bubble nucleus to a shock-scattering histotripsy pulse was computed with finite-strain elasticity incorporated in the Gilmore equation[7] in parallel with a first-order diffusion equation. The change in equilibrium bubble diameter due to gas transfer was assessed after the histotripsy pulse. The time for passive dissolution of the gas-filled bubble was computed following Neppiras.[9]

2. Methods

The radial oscillations of a cavitation nucleus in a viscoelastic medium were calculated by numerical integration. An adaptive fourth-order Runge-Kutta algorithm was implemented in MATLAB® (The Mathworks, Natick, MA) to solve a modified version of the Gilmore model

$$\left(1-\frac{\dot{R}}{C}\right)R\ddot{R}+\frac{3}{2}\left(1-\frac{\dot{R}}{3C}\right)\dot{R}^2=\left(1+\frac{\dot{R}}{C}\right)H+\frac{\dot{R}}{C}\left(1-\frac{\dot{R}}{C}\right)\frac{\mathrm{d}H}{\mathrm{d}R}, \tag{1}$$

where R is the time dependent bubble radius, the diacritic dot denotes the temporal derivative, and C is the sound speed in the medium at the bubble wall. The enthalpy, H, is defined in terms of the medium equation of state

$$H=\int_{P_\infty}^{P(R)}\left(\frac{P'+B}{A}\right)^{1/m}\mathrm{d}P', \tag{2}$$

[a)]Author to whom correspondence should be addressed.

where A, B, and m are defined following Lastman and Wentzell,[10] and P_∞ is the pressure far from the bubble wall. The pressure at the bubble wall, $P(R)$, is defined in terms of the surface tension σ, viscosity μ, shear modulus G, and gas pressure P_g

$$P(R) = P_g - \frac{2\sigma}{R} - \frac{4\mu\dot{R}}{R} - \frac{4G}{3}\left[1 - \left(\frac{R_0}{R}\right)^3\right]. \tag{3}$$

Soft tissues are the primary targets for histotripsy ablation. Thus, Eq. (3) varies from Church[7] through the addition of the last term to account for medium elasticity through the Kelvin-Voigt model. The diameter of the bubble nucleus, $2R_0$, was set to 20 nm to provide an upper estimate for the maximum diameter of histotripsy-induced cavitation.[11] The gas pressure is dependent on the time-varying number of moles of gas in the bubble n, and was computed following Church.[7] The molar-dependent equilibrium radius of the bubble, R_{0n}, was computed as

$$R_{0n} = \left[\frac{3k_B T n}{4\pi\left(P_0 + \frac{2\sigma}{R_0}\right)}\right]^{1/3}, \tag{4}$$

where k_B is Boltzmann's constant and T is the medium temperature. The following values were used for the medium properties: surface tension $\sigma = 0.056$ N/m,[12,13] dynamic viscosity $\mu = 0.005$ kg/m s,[12,13] shear modulus $G = 30$ kPa,[14] and temperature $T = 310$ K. The diffusion constant $D = 2.42 \times 10^{-9}$ m^2/s (Ref. 15) and saturated gas concentration $C_0 = 0.822$ mol/m^3 are required for computing the gas pressure, and were based on air dissolved in water. The gas concentration in the medium was set to 90%.[7] The shock-scattering histotripsy excitation term is embedded in P_∞, and was implemented with measured pressure waveforms of a 1-MHz fundamental frequency source.[11] Waveforms with peak negative/peak positive pressures over the range 14.5–18.3/88.9–107 MPa were utilized in the computations.

3. Results and discussion

3.1 Representative calculation

Examples of single cavitation nucleus response to a 3-cycle histotripsy pulse are shown in Fig. 1. The bubble expanded throughout the duration of the histotripsy excitation and underwent an inertial collapse. A damped oscillation of the bubble to the gas content-dependent equilibrium diameter followed the inertial collapse. The bubble contracted but did not collapse during the compressional phases of the histotripsy pulse, consistent with previous experimental observations[3] and computations.[11] The maximum bubble diameter at the completion of the histotripsy excitation increased 10 μm (15%) for computations accounting for gas diffusion compared to computations that did not incorporate the effects of diffusion. These results denote diffusion has minimal influence on the bubble dynamics during the excitation, consistent with computations of shock wave lithotripter-induced cavitation.[7]

Despite its minor contribution to the maximum bubble diameter, significant gas influx occurred during the bubble expansion. The gas content of the bubble

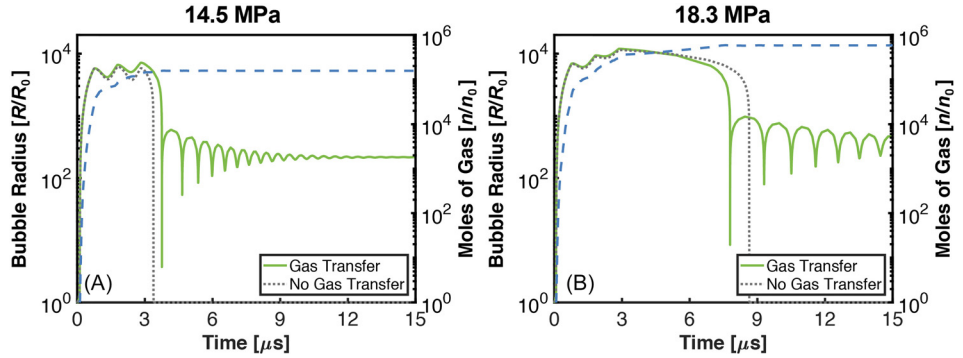

Fig. 1. (Color online) The normalized bubble radius as a function of time (solid green curve for calculations with diffusion, dotted gray curve calculations without diffusion. Left ordinate for both curves), and the corresponding number of moles of gas in the bubble (dashed blue curve, right ordinate). (A) 14.5 MPa/88.9 MPa peak positive/peak positive histotripsy pulse, (B) 18.3 MPa/107 MPa peak positive/peak positive histotripsy pulse. The duration of the histotripsy pulse was 3 cycles with a fundamental frequency of 1 MHz, and the diameter of the bubble nucleus was 20 nm.

increased by over 5 orders of magnitude during the histotripsy insonation, an order of magnitude larger than a computation utilizing a shock wave lithotripter excitation.[7] Bubble expansion initiated by the histotripsy pulse, and the resulting gas diffusion, would be mitigated by the elastic medium compared to the fluid medium considered in the shock wave lithotripter study.[16] The increased gas flow observed in this study may be due to the excitation waveform. The lithotripter pulse was compressional leading, causing the bubble to collapse during the initial portions of the tensile phase. The histotripsy pulse used in this study was tensile leading, and bubble expansion was observed throughout the duration of the histotripsy pulse. While the inertia of shock-induced bubble contraction must be overcome prior to in-gassing for lithotripter pulses, bubble expansion-induced gas influx occurs throughout the histotripsy pulse considered in this study.

After the histotripsy excitation, the bubble underwent an inertial collapse. For computations accounting for diffusion, the gas content buffered the bubble collapse compared to computations neglecting diffusion. The bubble diameter at the completion of the collapse was increased by over 3 orders of magnitude when comparing calculations with and without diffusion [Fig. 2(B)]. In computations with diffusion, the influx of gas prevented the bubble from contracting below the size of the original nucleus during the collapse phase. The size of the bubble during the final stages of contraction increased with the peak negative pressure of the pulse, similar to the behavior of lithotripsy induced cavitation.[7]

The hallmark of histotripsy liquefaction is strain induced by expansion and contraction of the bubble relative to the size of its nucleus.[17] The lack of bubble contraction below the nucleus size indicates compression-only strain. The bubble wall speed is another metric of the inertial collapse, and was reduced by more than 3 orders of magnitude when comparing computations with and without diffusion [Fig. 2(C)]. The strain rate is proportional to the bubble wall speed and dictates the morphology and extent of cell death.[18] The reduction in both the strain and strain rate of the bubble collapse in the presence of diffusion may indicate compressional strains associated with bubble expansion to be a dominant mechanism for histotripsy-induced tissue liquefaction in gaseous tissues.[11]

The fate of the bubble following the inertial collapse is unknown. Mitigation of the inertial collapse due to diffusion may prevent splintering of the bubble into smaller daughter bubbles, prompting the bubble to rebound and undergo a damped oscillation to the gas content-dependent equilibrium size. It is assumed here that the non-splintered, gas-filled bubble is the source of persistent cavitation observed between consecutive histotripsy pulses. The gas content-dependent equilibrium diameter at the completion of the histotripsy pulse was between 0.95 and 1.46 μm [Fig. 2(A)]. The equilibrium diameters computed in this study are smaller than that computed for lithotripsy excitations with similar peak negative pressures (equilibrium diameter of 80 μm for 16 MPa).[7] The discrepancy may be due to the 20 nm nucleus considered in this study in comparison to the 2–20 μm nucleus considered previously. Nanoscale nuclei are intrinsic to the tissue targets of histotripsy,[19,20] whereas micrometer-sized nuclei can be harbored on a kidney stone.[21] Despite the difference in equilibrium size between the two sources of nuclei, the bubbles computed in this study are large enough to be visualized with B-mode ultrasound.[22] Passive dissolution of the gas-filled residual bubbles would require between 15 and 58 ms.[9] Experimental observations indicate histotripsy-induced cavitation persists for 30 to 50 ms post insonation,[4–6] consistent with these calculations.

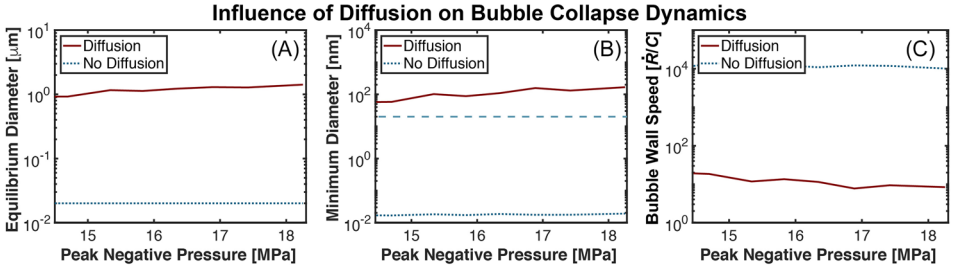

Fig. 2. (Color online) (A) Change in equilibrium bubble diameter as a function of the peak negative pressure. (B) Minimum bubble size during the final stages of collapse as a function of the peak negative pressure. For reference, the size of the original bubble nucleus (20 nm) is demarked with the blue, long-dashed curve. (C) Bubble wall speed during the final stages of collapse, normalized to the medium sound speed C (1540 m/s). The acoustic excitation was a 3-cycle histotripsy pulse with a fundamental frequency of 1 MHz. The size of the bubble nucleus was 20 nm. Calculations with and without gas diffusion are noted in the legend.

The application of histotripsy pulses prior to bubble dissolution cause incomplete liquefaction of the focal zone.[23] Based on the dissolution times computed in this study, residual cavitation would be present when the pulse repetition frequency was between 16 and 66 Hz. In practice, residual cavitation is mitigated when the pulse repetition frequency was less than 1 Hz.[23] The discrepancy may be due to the single bubble computations in this study. The histotripsy pulse will form a bubble cloud,[3] and bubbles within the cloud may coalesce. The larger, coalesced bubbles would require a correspondingly longer time for dissolution.[9] Regardless, passive diffusion is a slow process, prompting the development of insonation schemes for acoustically-driven diffusion.[24,25]

3.2 Dependence of the equilibrium bubble size with pulse duration

Shock-scattering histotripsy pulses require multiple cycles for efficacious ablation, and the diffusion rate varies throughout the pulse. The largest influx of gas occurred during the first cycle of the pulse (Fig. 3). Gas diffusion would thus also contribute to bubble persistence during intrinsic-threshold histotripsy, a form of histotripsy that utilizes a single-cycle excitation.[19] Beyond the first cycle, the growth rate of the equilibrium bubble diameter reduced and was dependent on the peak negative pressure. For the largest peak negative pressure considered here (18.3 MPa), the equilibrium bubble diameter was 0.8 and 1.9 μm at the completion of 1 and 5 cycle pulses, respectively. Although the equilibrium bubble size increased only 1.1 μm over this range of pulse durations, the time for passive dissolution increased by 185 ms (15 and 200 ms for 1 and 5 cycle pulses, respectively). Pulse duration is thus also a consideration when avoiding bubble persistence.

3.3 Influence of saturated gas pressure on equilibrium bubble size

The equilibrium diameter dependence on the degree of medium gas saturation is shown in Fig. 4(A). The equilibrium bubble diameter at the completion of the 3-cycle pulse varied by more than a factor of 2 over the range of 10%–110% gas saturation (0.7 μm vs 1.5 μm at peak negative pressure 18.3 MPa). The time for passive dissolution of a 0.7 μm bubble in a 10% gas saturated medium would be 5.3 ms, and 63.4 ms at 110% gas saturation for a 1.5 μm bubble [Fig. 4(B)].

The lower range of medium gas saturations explored in this study would not occur physiologically,[26] even in ischemic tissues.[27] However, *in vitro* studies of histotripsy utilize phantoms of highly degassed agar to monitor bubble dynamics.[6,28,29] As noted in Fig. 4(A), the equilibrium diameter, and therefore the duration of bubble persistence, is reduced in degassed media compared to physiologic gas saturated media. Thus, inference of the bubble lifetime in a degassed phantom may not be totally reflective of *in vivo* bubble activity.

4. Conclusions

In this study, an established model of bubble dynamics[7] was utilized to investigate the influence of gas diffusion on shock-scattering histotripsy-induced cavitation. While little difference was observed in the bubble dynamics during the histotripsy excitation, the influx of gas buffered the collapse of the bubble compared to calculations without gas transfer. The equilibrium bubble diameters computed in this study based on

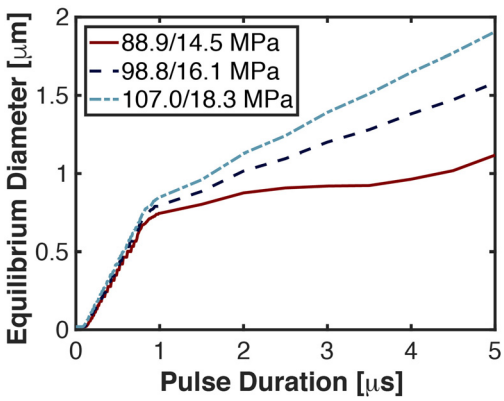

Fig. 3. (Color online) Equilibrium bubble diameter at the completion of the histotripsy pulse as a function of the pulse duration. The diameter of the bubble nucleus was 20 nm, and the fundamental frequency of the histotripsy excitation was 1 MHz. The peak positive/peak negative pressure of the excitation is noted in the legend.

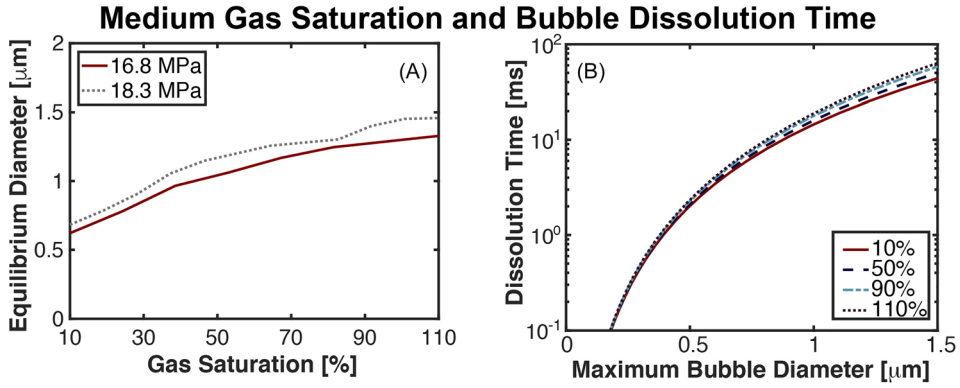

Fig. 4. (Color online) (A) Change in equilibrium bubble size as a function of the dissolved gas concentration relative to the saturated gas pressure at the completion of a three-cycle histotripsy pulse. The peak negative pressure of the histotripsy pulse is noted in the legend. A 20-nm nucleus was used for the computations shown here, and the excitation was had a fundamental frequency of 1 MHz. (B) Bubble dissolution time as a function of the maximum bubble diameter parametric with the dissolved gas concentration.

shock-scattering excitations were more than an order of magnitude greater than the cavitation nucleus, and would require more than 15 ms to re-condense under passive diffusion. Overall, these results indicate diffusion is an important aspect on the longevity of histotripsy cavitation.

There are several aspects of this study that limit the generalizability of these findings. The amplitude of the measured shock scattering histotripsy pulses used as the source term in Eq. (2) may be underestimated due to spatial averaging of the fiber width and the bandwidth of the system.[30] The size of the bubble is assumed to be much smaller than the wavelength of the excitation pressure for the Gilmore equation, which is not the case for shock wave excitation. The oscillations of a single bubble were considered in this study, which can be used to gauge the onset of shock scattering-induced bubble cloud formation.[11] These computations neglect the bubble-bubble interactions that occur in a dense cloud. Shock-scattering pulses up to 20 μs in duration have been utilized.[31] The longest pulses considered here were 5 μs in duration due to the large computational time ($\sim$20 h/calculation). Additional effects, such as the transfer of vapor, were not considered in these calculations,[32] and the assumptions of air as the gas content may not be appropriate in some physiologic conditions, particularly in ischemic environments.[27] Nevertheless, these findings indicate diffusion in an important aspect of histotripsy-induced cavitation.

Acknowledgments

The authors gratefully acknowledge the fruitful discussion with Adam Maxwell and Eli Vlaisavljevich. This work was funded in part by the National Institutes of Health, Grant Nos. K12CA139160 and R01HL13334.

References and links

[1]V. A. Khokhlova, J. B. Fowlkes, W. W. Roberts, G. R. Schade, Z. Xu, T. D. Khokhlova, T. L. Hall, A. D. Maxwell, Y. N. Wang, and C. A. Cain, "Histotripsy methods in mechanical disintegration of tissue: Towards clinical applications," Int. J. Hyperthermia **31**(2), 145–162 (2015).
[2]Z. Xu, A. Ludomirsky, L. Y. Eun, T. L. Hall, B. C. Tran, J. B. Fowlkes, and C. A. Cain, "Controlled ultrasound tissue erosion," IEEE Trans. Ultrason., Ferroelect., Freq. Contr. **51**(6), 726–736 (2004).
[3]A. D. Maxwell, T. Y. Wang, C. A. Cain, J. B. Fowlkes, O. A. Sapozhnikov, M. R. Bailey, and Z. Xu, "Cavitation clouds created by shock scattering from bubbles during histotripsy," J. Acoust. Soc. Am. **130**(4), 1888–1898 (2011).
[4]F. Prieur, A. Zorgani, S. Catheline, R. Souchon, J.-L. Mestas, M. Lafond, and C. Lafon, "Observation of a cavitation cloud in tissue using correlation between ultrafast ultrasound images," IEEE Trans. Ultrason., Ferroelect., Freq. Contr. **62**(7), 1256–1264 (2015).
[5]Z. Xu, T. L. Hall, J. B. Fowlkes, and C. A. Cain, "Effects of acoustic parameters on bubble cloud dynamics in ultrasound tissue erosion (histotripsy)," J. Acoust. Soc. Am. **122**(1), 229–236 (2007).
[6]K. B. Bader, K. J. Haworth, A. D. Maxwell, and C. K. Holland, "Post hoc analysis of passive cavitation imaging for classification of histotripsy-induced liquefaction in vitro," IEEE Trans. Med. Imag. **37**(1), 106–115 (2018).
[7]C. C. Church, "A theoretical study of cavitation generated by an extracorporeal shock wave lithotripter," J. Acoust. Soc. Am. **86**, 215–227 (1989).
[8]W. Kreider, A. D. Maxwell, T. Khokhlova, J. C. Simon, V. A. Khokhlova, O. Sapozhnikov, and M. R. Bailey, "Rectified growth of histotripsy bubbles," Proc. Mtgs. Acoust. **19**, 075035 (2013).
[9]E. A. Neppiras, "Acoustic cavitation," Phys. Rep. **61**(3), 159–251 (1980).

[10]G. J. Lastman and R. A. Wentzell, "Comparison of five models of spherical bubble response in an inviscid compressible liquid," J. Acoust. Soc. Am. **69**(3), 638–642 (1981).
[11]K. B. Bader and C. K. Holland, "Predicting the growth of nanoscale nuclei by histotripsy pulses," Phys. Med. Biol. **61**(7), 2947–2966 (2016).
[12]C. C. Church, C. Labuda, and K. Nightingale, "A theoretical study of inertial cavitation from acoustic radiation force impulse imaging and implications for the mechanical index," Ultrasound Med. Biol. **41**(2), 472–485 (2015).
[13]C. K. Holland and R. E. Apfel, "Improved theory for the prediction of microcavitation thresholds," IEEE Trans. Ultrason., Ferroelect., Freq. Contr. **36**(2), 204–208 (1989).
[14]R. Cao, Z. Huang, T. Varghese, and G. Nabi, "Tissue mimicking materials for the detection of prostate cancer using shear wave elastography: A validation study," Med. Phys. **40**(2), 022903 (2013).
[15]L. A. Crum and G. M. Hansen, "Generalized equations for rectified diffusion," J. Acoust. Soc. Am. **72**(5), 1586–1592 (1982).
[16]K. B. Bader, "The influence of medium elasticity on the prediction of histotripsy-induced bubble expansion and erythrocyte viability," Phys. Med. Biol. **63**(9), 095010 (2018).
[17]L. Mancia, E. Vlaisavljevich, Z. Xu, and E. Johnsen, "Predicting tissue susceptibility to mechanical cavitation damage in therapeutic ultrasound," Ultrasound Med. Biol. **43**(7), 1421–1440 (2017).
[18]E. Bar-Kochba, M. T. Scimone, J. B. Estrada, and C. Franck, "Strain and rate-dependent neuronal injury in a 3D *in vitro* compression model of traumatic brain injury," Sci. Rep. **6**, 30550–30561 (2016).
[19]A. D. Maxwell, C. A. Cain, T. L. Hall, J. B. Fowlkes, and Z. Xu, "Probability of cavitation for single ultrasound pulses applied to tissues and tissue-mimicking materials," Ultrasound Med. Biol. **39**(3), 449–465 (2013).
[20]E. Vlaisavljevich, K.-W. Lin, A. D. Maxwell, M. T. Warnez, L. Mancia, R. Singh, A. J. Putnam, J. B. Fowlkes, E. Johnsen, C. Cain, and Z. Xu, "Effects of ultrasound frequency and tissue stiffness on the histotripsy intrinsic threshold for cavitation," Ultrasound Med. Biol. **41**(6), 1651–1667 (2015).
[21]J. C. Simon, O. A. Sapozhnikov, W. Kreider, M. Breshock, J. C. J. Williams, and M. R. Bailey, "The role of trapped bubbles in kidney stone detection with the color Doppler ultrasound twinkling artifact," Phys. Med. Biol. **63**(2), 025011 (2018).
[22]T. L. Szabo, *Diagnostic Ultrasound Imaging: Inside Out* (*Biomedical Engineering*), 1st ed. (Academic Press, Waltham, MA, 2004).
[23]T.-Y. Wang, Z. Xu, T. L. Hall, J. B. Fowlkes, and C. A. Cain, "An efficient treatment strategy for histotripsy by removing cavitation memory," Ultrasound Med. Biol. **38**(5), 753–766 (2012).
[24]A. P. Duryea, W. W. Roberts, C. A. Cain, H. A. Tamaddoni, and T. L. Hall, "Acoustic bubble removal to enhance SWL efficacy at high shock rate: An *in vitro* study," J. Endourol. **28**(1), 90–95 (2014).
[25]A. P. Duryea, W. W. Roberts, C. A. Cain, and T. L. Hall, "Removal of residual cavitation nuclei to enhance histotripsy erosion of model urinary stones," IEEE Trans. Ultrason., Ferroelect., Freq. Contr. **62**(5), 896–904 (2015).
[26]M. T. Lategola, "Measurement of total pressure of dissolved gas in mammalian tissue in vivo," J. Appl. Physiol. **19**(2), 322–324 (1964).
[27]A. J. Brooks, J. Eastwood, I. J. Beckingham, and K. J. Girling, "Liver tissue partial pressure of oxygen and carbon dioxide during partial hepatectomy," Br. J. Anaesth. **92**(5), 735–737 (2004).
[28]A. D. Maxwell, T. Y. Wang, L. Yuan, A. P. Duryea, and Z. Xu, "A tissue phantom for visualization and measurement of ultrasound-induced cavitation damage," Ultrasound Med. Biol. **36**(12), 2132–2143 (2010).
[29]E. Vlaisavljevich, Y. Kim, G. Owens, W. Roberts, C. Cain, and Z. Xu, "Effects of tissue mechanical properties on susceptibility to histotripsy-induced tissue damage," Phys. Med. Biol. **59**(2), 253–270 (2013).
[30]M. S. Canney, M. R. Bailey, L. A. Crum, V. A. Khokhlova, and O. A. Sapozhnikov, "Acoustic characterization of high intensity focused ultrasound fields: A combined measurement and modeling approach," J. Acoust. Soc. Am. **124**(4), 2406–2420 (2008).
[31]A. Maxwell, Z. Xu, B. Fowlkes, O. Sapozhnikov, C. Cain, M. Bailey, V. Khokhlova, and L. Crum, "Disintegration of tissue using high intensity focused ultrasound: Two approaches that utilize shock waves," Acoust. Today **8**(4), 24–37 (2012).
[32]W. Kreider, L. A. Crum, M. R. Bailey, and O. A. Sapozhnikov, "A reduced-order, single-bubble cavitation model with applications to therapeutic ultrasound," J. Acoust. Soc. Am. **130**(5), 3511–3530 (2011).